Cement and Concrete Research 40 (2010) 313–320

Contents lists available at ScienceDirect

Cement and Concrete Research

journal homepage: http://ees.elsevier.com/CEMCON/default.asp

Photocatalytic degradation of air pollutants — From modeling to large scale application

M. Hunger [a,*], G. Hüsken [a], H.J.H. Brouwers [a,b]

[a] Department of Construction Management and Engineering, Faculty of Engineering Technology, University of Twente, P.O. Box 217, 7500 AE, Enschede, The Netherlands
[b] Department of Architecture, Building and Planning, Eindhoven University of Technology, P.O. Box 531, 5600 MB Eindhoven, The Netherlands

ARTICLE INFO

Article history:
Received 11 March 2009
Accepted 18 September 2009

Keywords:
Photocatalysis
(A) Reaction
(A) Kinetics
(C) Diffusion
(E) Modeling

ABSTRACT

Indoor as well as outdoor air quality and their limiting values remain a major problem to our present-day society.
This paper addresses the modeling of the decomposition process of nitrogen monoxide (NO) on reactive concrete surfaces under the controlled exposition of a UV source. Within this model the external mass transfer of the pollutant and the internal molecule diffusion-reaction were considered. A first-order kinetics equation is derived with respect to the NO concentration and a site-competitive adsorption between NO/NO_2 and water molecules, resulting in a dependence of the reaction kinetics on the relative humidity. Using the proposed model, a reaction rate constant k and an adsorption equilibrium constant K_d can be derived which describe an active paving stone accurately. Experimental results from a self-developed photoreactor with continuous flow mode were used to validate the proposed kinetic expression. Furthermore, the effect of variations in process conditions such as irradiance and relative humidity on the two constants k and K_d is investigated. All modeling work provides a sound foundation for the translation of this process to real outside conditions. In this regard an upcoming project in a Dutch city is described in brief.
© 2009 Elsevier Ltd. All rights reserved.

1. Introduction

In order to overcome atmospheric pollution problems, a number of removal techniques are available. Mostly these are filter systems taking the respective pollutant from the gaseous phase and transforming it into another state which is stored and accumulated. This actually is only a shift of the problem. Since about 10 years, however, literature increasingly reports about a process, the so-called photocatalytic oxidation (PCO), using a solid semiconductor catalyst activated by UV-radiation. These systems are already available in active filter devices and their reaction kinetics on certain pollutants is sufficiently described. Therefore, such tailor-made reactor systems can be applied to systematically improve local problems such as in office buildings or along production sites.

However, there is no large-scaled solution for outdoor application such as in highly frequented inner city areas yet. Therefore the use of photocatalytic active concrete paving blocks appears to be one of the most serious attempts to control air quality in terms of e.g. nitrogen oxide (NOx) contamination in congested urban areas. Although these concrete products are already commercially available, hardly anything concerning their reaction kinetics has been published yet.

PCO has now been applied to construction materials for more than a decade. The general mode of action of photocatalysis itself is already known since a much longer time. However, since Honda and Fujishima introduced the water decomposition phenomenon (Honda–Fujishima Effect) of a photoelectrochemical cell using a titanium oxide photo electrode, photocatalysts have attracted extensive interest [1]. Wastewater treatment especially in regard to pharmaceutical and diagnostic media residues [2] but also the treatment of waste water from dyeing factories [3] set a new motivation for further research. In construction industry the window pane was probably the first product coming on the market equipped with photocatalytic properties. But now also cementitious binders are combined with titanium dioxide in order to attach them with air-purifying and self-cleaning effects. The last mentioned feature actually was the original intention whereas the former was rather a side effect, discovered later.

In the air-purifying sense this chemical process is particularly effective when large connected surface areas (horizontal or vertical), preferably as close as possible to the pollutant source are equipped with photocatalytically active materials. Examples of pollutants which can be eliminated are numerous. It can be said that all natural organic matter (NOM), including hardly oxidizable organic compounds, volatile organic compounds (VOCs) such as benzene, aldehydes and toluene, and a variety of inorganic compounds such as NO_x, SO_x and NH_3 can be oxidized. This paper will focus on the degradation performance of NO and more specifically on its

* Corresponding author. Tel.: +31 53 489 6863; fax: +31 53 489 2511.
E-mail address: martinhunger@gmx.at (M. Hunger).

0008-8846/$ – see front matter © 2009 Elsevier Ltd. All rights reserved.
doi:10.1016/j.cemconres.2009.09.013

modeling. Nitrogen oxides are besides carbon dioxide, sulfur dioxide, gaseous ammonia, ozone and particulate matter the most critical pollutants of the present air quality. Furthermore, NO can be handled with ease in the lab and its detection and analysis does not require very complex test facilities.

Because of the preferred large-scale application mentioned above, the concrete paving stone has become one of the most recognized construction elements providing photocatalytic properties so far. These active paving stones are commercially available for a fairly long time. Their market launch was, first in Japan, at the end of the 1990th. Since then their efficiency was analyzed in several scientific papers. In [4] a comparative study was presented, analyzing a representative share of the active paving stones available from the European market. Furthermore, a measuring procedure was proposed allowing for device independent and comparative test results. The major conclusion of this investigation was that independent and comparative control is essential to evaluate the broad variety of available products which again show a wide range in efficiency.

A next major step in understanding and deeper analyzing PCO is the modeling of its reaction kinetics, which actually is the focus of this paper. Here the literature provides a large number of papers dealing with the reaction kinetics of the photocatalytic oxidation of VOCs in specially designed gas reactors. [5] for example describes the degradation of formaldehyde which is a typical indoor VOC, extensively existing in modern building materials and household products. The degradation of Trichloroethylene (TCE), an often used degreaser and solvent, was modeled by [6]. In [7], [8] and [9] the degradation of perchloroethylene (PCE), a substance similar to TCE but more critical due to its manifold decomposition products, is modeled. For a detailed discussion of the reaction pathways for photocatalytic oxidation of nitrogen monoxide to nitric acid (HNO_3) over TiO_2, the reader is referred to [17]. Here also the transient intermediates such as nitrogen dioxide (NO_2) are addressed and their influence is investigated. This selection proofs that the modeling of PCO reaction kinetics is sufficiently accounted for in research. However, all mentioned papers refer to reactor setups which have been specifically designed for the purpose of treating polluted air. Most authors used the Langmuir–Hinshelwood model to evaluate the photocatalytic degradation rate of the respective pollutants. To the authors' knowledge, there are no papers addressing the reaction kinetics of active concrete paving stones yet. This is important for the understanding and optimization of these products, and therefore this will be developed in the present paper. Furthermore, also influencing factors such as relative humidity and irradiance level are incorporated in the presented model. Finally, a brief introduction will be given on an ongoing large-scale pilot project, where the lab based modeling experience is tried to be translated into real scale.

2. Experimental description

In order to perform modeling work, a constant and controlled test environment as well as a suitable sample needs to be available. As mentioned before, there are a number of photocatalytic concrete paving blocks available on the market. From a comparative study on active paving stones presented by [4] the stone with the highest efficiency was selected for further modeling experiments. It is believed that tests with highly reactive surfaces can reveal smaller deviations in the degradation rate, which would not become as obvious when testing samples with a generally lower degradation capability. The sample, an active paving block of the dimension 100×200 mm^2, is described in [4]. Here also the test setup, which was designed for tests on active paving stones, is described in more detail. The used reactor operates in steady state. It houses the paving stone in such a way that the polluted gas can only touch it along the reactive surface but due to the immediate diffusion of the reactant it can be modeled as a plug flow reactor. The flow of gas along the planar reaction surface is laminar and is conducted in a duct of variable height which is at the lower side limited by the paving stone surface and from above by a borosilicate glass pane. If not otherwise stated the slit height h amounts to 3 mm. The Reynolds number of the flow reads:

$$Re = \frac{v_{air} d_h \rho_{air}}{\mu_{air}} = \frac{2 v_{air} h \rho_{air}}{\mu_{air}} = \frac{2Q}{B v_{air}}, \quad (1)$$

d_h is the hydraulic diameter of the considered channel, defined as four times the cross-sectional area divided by the perimeter. For the slit considered here, $d_h = 2\,h$. Substituting $Q = 3$ l/min, $B = 100$ mm and $v_{air} = 1.51\cdot10^{-5}$ m^2/s (1 bar, 20 °C) yields $Re \approx 65$. This low Reynolds number implies that the flow within the reactor cell is laminar. A fully developed parabolic velocity profile will be developed at $L_d = 0.05\,Re\,2\,h$, so here $L_d \approx 20$ mm [10]. That means that only the first 10% of the slit length are influenced by entrance effects. In the remaining 90% of the reactor cell a fully developed laminar flow profile exists. Despite the laminar flow along only one reactive surface, the duct volume can be considered as a plug flow reactor. FEM models show that a concentration gradient will only develop in flow direction. The difference of the reactant along the height axis can be neglected due to the immediate diffusion. Experimental results underline this assumption.

A schematic diagram of the reactor cell is given in Fig. 1. The light intensity E is kept constant at 10 W/m^2 (300–400 nm). In Table 1 the applied process conditions are summarized.

3. Modeling

The following section refers to the modeling of the reaction kinetics. Parts of this section are already published in [11]. First, one should observe the general course of the multistage reaction. This reaction starts with the diffusion of NO at the concrete surface and continues with the conversion to NO_x. This means that the process contains two transfer steps, the mass transfer from gas to wall and the conversion at the active concrete surface. In line with findings by [12], and [13], it will be demonstrated that the conversion is the rate limiting step.

The NO mass flux from gas to adsorbing surface can be described by:

$$\dot{m} = \frac{ShD}{d_h}(C_g - C_w) = \frac{ShD}{2h}(C_g - C_w), \quad (2)$$

with d_h, as hydraulic diameter, and C_g (mean mixed or bulk in gaseous phase) and C_w (on the surface) are the NO concentrations (in mg NO per m^3 air). The relation between C_g and C_{con} is as follows:

$$C_g = \frac{M_{NO}\rho_{air}}{M_{air}} C_{con}. \quad (3)$$

Considering that the molecular mass of the deployed synthetic air (M_{air}) is 28.8 g/mole (80% M_{N2} and 20% M_{O2}), that of NO (M_{NO}) is 30.0 g/mole, and that ρ_{air} is 1.204 kg/m^3, it follows that C_g (in mg/m^3)

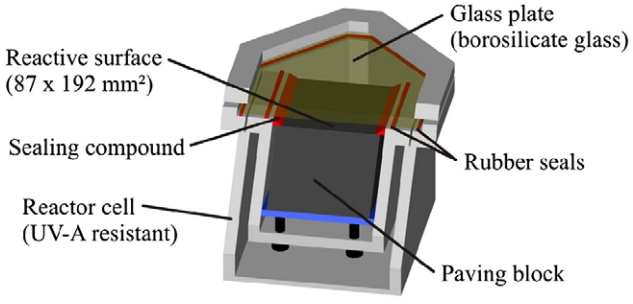

Fig. 1. Schematic diagram of the reactor cell.

Table 1
Summary of the process conditions during measurements.

Operating conditions	Value
Feed flow rate	1, 3 and 5 l/min
Flow velocity above reactive surface	0.056, 0.167 and 0.278 m/s
Temperature	20 °C
Pressure	101,325 kPa
NO inlet concentration	0.1, 0.3, 0.5, 1.0 ppmv (or 0.125, 0.376, 0.627 and 1.254 mg/m^3)
Relative humidity	50%
Reactive surface	87×192 = 17,139 mm^2
Irradiance (300–400 nm)	10 W/m^2

is about 1.254 C_{con} (in 10^{-6} mol/mol = ppmv). These calculations are based on standard conditions which define $T = 293.15$ K and $p = 101.325$ kPa = 1 atm.

Sh from Eq. (2) refers to the Sherwood number, which in thermodynamics gives the ratio of convective to diffusive mass transport. For slits with one inert and one exchanging side, the side walls are neglected, *Sh* amounts to about 5 [14]. Furthermore, *D* the diffusion coefficient of NO in air can be estimated to be $1.51 \cdot 10^{-5}$ m^2/s, which is the kinematic viscosity of air (υ_{air}).

3.1. Diffusion as limiting step

Now it is assumed that the diffusion of NO from the gaseous phase to the concrete surface is the limiting step. This implies a complete and instantaneous conversion which would turn the NO concentration at the surface to zero. The NO mass balance equation then reads:

$$v_{air} h \frac{dC_g}{dx} = -\dot{m} = -\frac{ShD}{2h} C_g, \tag{4}$$

with as boundary condition:

$$C_g = C_{g,in}, \tag{5}$$

Integrating Eq. (4) and application of Eq. (5) yields:

$$\frac{C_{g,out}}{C_{g,in}} = e^{-\frac{ShDL}{2v_{air}h^2}}, \tag{6}$$

with $C_{g,out} = C_g(x = L)$ and L being the length of the active surface, which is 192 mm in this case. The variable h describes the height of the plug flow reactor volume, i.e. the slit height in that case (cp. Fig. 1). Substituting all variables, including $v_{air} = 0.17$ m/s and $h = 3$ mm, into Eq. (6) yields $C_{g,out}/C_{g,in} \approx 0.007$. In other words, in the case that the diffusion to the wall would be the rate limiting step, the exit concentration would be close to 1% of the inlet concentration, i.e. 99.3% of the NO would be converted. However, the present measurements and also previous research [4] learned this is not the case, so that the conversion rate at the surface cannot be ignored (cp. Tables 2 and 3).

Table 2
NO outlet concentrations of the reactor considering varying inlet concentrations and flow rates for the photocatalysis of the paving stone example.

C_{in} [ppmv]	C_{out} Volumetric flow rate Q [l/min]			NO_x removal rate [%] Volumetric flow rate Q [l/min]		
	1	3	5	1	3	5
0.1	0.011	0.032	0.041	89.0	68.4	59.4
0.3	0.039	0.157	0.197	87.1	47.6	34.3
0.5	0.210	0.309	0.356	58.0	38.3	28.9
1.0	0.334	0.729	0.779	66.6	27.1	22.1

Table 3
NO outlet concentrations and removal rates of the reactor considering constant inlet concentration $C_{in} = 0.3$ ppmv but varying flow rates and slit heights.

Slit height [mm]	C_{out} Volumetric flow rate Q [l/min]			NO_x removal rate [%] Volumetric flow rate Q [l/min]		
	1	3	5	1	3	5
2	0.093	0.162	–	68.8	46.1	–
3	0.039	0.157	0.197	87.1	47.6	34.3
4	0.065	0.157	0.183	78.3	47.6	39.1

3.2. Conversion as limiting step

In the following, it is now a priori assumed that the conversion is the rate limiting step, so that C_w now equals C_g, which will be verified below.

For the prevailing photocatalytic gas–solid surface reaction, only adsorbed NO can be oxidized. In the past therefore the Langmuir–Hinshelwood rate model has been widely used, e.g. by [5,6,12,13,15] as well as [16], and will also be applied here. Following this model, the disappearance rate of reactant reads:

$$r_{NO} = \frac{kK_d C_g}{1 + K_d C_g}, \tag{7}$$

with k as reaction rate constant (mg/m^3 s) and K_d as the adsorption equilibrium constant (m^3/mg). The NO balance equation now reads:

$$v_{air} \frac{dC_g}{dx} = -r_{NO} = -\frac{kK_d C_g}{1 + K_d C_g}, \tag{8}$$

Integration and using the boundary condition, Eq. (5), yields:

$$\frac{1}{k} + \frac{1}{kK_d} \frac{\ln\left(\frac{C_{g,in}}{C_{g,out}}\right)}{(C_{g,in} - C_{g,out})} = \frac{L}{v_{air}(C_{g,in} - C_{g,out})} = \frac{V_{reactor}}{Q(C_{g,in} - C_{g,out})}, \tag{9}$$

with $V_{reactor} = LBh$ and $Q = v_{air}Bh$, and again, $C_{g,out} = C_g(x = L)$. In Table 2 this $C_{g,out}$ of the experiments with the paving stone is summarized.

The inlet concentration $C_{g,in}$ had values of 0.1, 0.3, 0.5 and 1 ppmv NO (or 0.125, 0.376, 0.627 and 1.254 mg/m^3), and the flow rate Q was 1, 3 and 5 l/min.

3.3. Validation of the model

In Fig. 2, $y = V_{reactor}/Q(C_{g,in} - C_{g,out})$ is set out versus $x = \ln(C_{g,in}/C_{g,out})/(C_{g,in} - C_{g,out})$, and the data fit with the line $y = (1.19\ \text{s})x + 2.37\ \text{m}^3\text{s/mg}$. The intersection with the ordinate corresponds to $1/k$, so that $k = 0.42$ mg/m^{3}s, and the slope to $1/kK_d$, so that $K_d = 2.00$ m^3/mg.

Reviewing the relevant literature, to the knowledge of the authors, no such data on the photocatalysis of concrete can be found. In [16] obtained $k = 6.84$ mg/m^{3}s and $K_d = 1.13$ m^3/mg was gained for the NO degradation by woven glass fabrics, their NO inlet concentration being in the range 40–80 ppmv. Concerning the photocatalytic ammonia degradation by cotton woven fabrics, [13] obtained $k = 0.10$ mg/m^{3}s and 0.24 mg/m^{3}s, and $K_d = 0.035$ m^3/mg and 0.112 m^3/mg, whereby the NH_3 inlet concentration ranged from 14 to 64 mg/m^3. With an in principle similar reactor (one reactive surface but no packed bed) [17] obtained a K_d of about 1.1 m^3/mg, applying NO levels from 5 to 60 ppm. As can be seen from this brief literature review, the respective constants vary as expected but are located in the same order of magnitude. It is assumed that the photocatalytic oxidation of NO is exclusively promoted by TiO_2, therefore the constants should be similar. However, the boundary conditions broadly vary and cannot be compared from experiment to experiment. Therefore, also the cross-check of literature values with each other does not lead to matches. The influence of the light spectrum, the type of TiO_2,

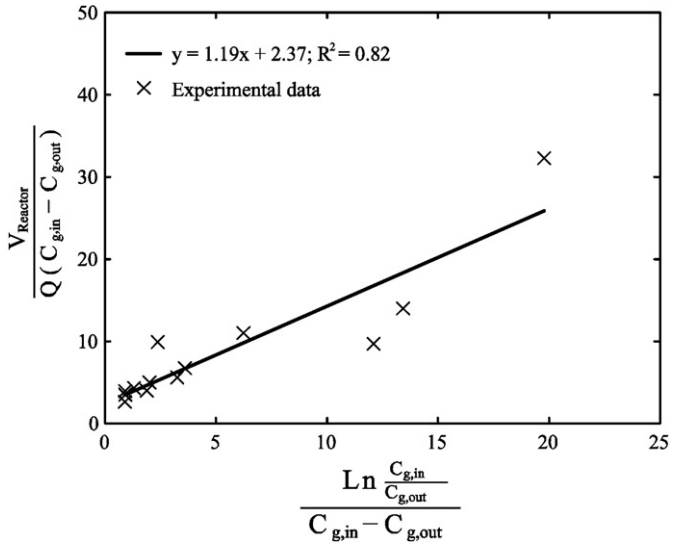

Fig. 2. Regression results of data presented in Tables 2 and 3 for the photocatalysis of the paving stone example.

surface roughness of the paving sample and the catalyst concentration, to only mention a few, is at this moment too complex to be fully considered in a model to be developed.

With the obtained values of k and K_d the conversion rate and diffusion rate can be compared. Dividing the conversion/transfer rates as governed by Eqs. (8) and (4) yields kK_d2h^2/ShD, and substituting the prevailing values reveals that this ratio is about 0.2, i.e. the diffusion rate is about five times the conversion rate. Note that the employed kK_d is an upper limit for $kK_d/(1+K_dC_g)$, so that the actual ratio will even be smaller. From this small conversion/transfer rate ratio one can conclude that indeed the degradation rate is much lower than the diffusion rate, and hence it is the limiting rate. This is also confirmed by [18] who found conversion rates proportionally increasing with the specific surface area of the applied titanium dioxide. In [17] the external mass transfer is also not identified to be the limiting step.

In the present research this fact was furthermore investigated by executing experiments with varied slit heights of 2 and 4 mm, besides the standard 3 mm. When the assumption of a mainly conversion controlled process with a high diffusion rate is indeed true, then a change in the slit height should not influence the degradation performance. $C_{g,in}$ was now taken as 0.376 mg/m^3 (0.3 ppmv) and the flow rate Q was 1, 3 and 5 l/min. In Table 3, and also in Fig. 2, this data is included. Except for the smallest flow rate ($Q=1$ l/min), the degradation rates match well with the values listed in Table 2, and the computed $V_{reactor}/Q(C_{g,in}-C_{g,out})$ and $\ln(C_{g,in}/C_{g,out})/(C_{g,in}-C_{g,out})$ are also compatible with the previous ones set out in Fig. 2 and the fitted trend line.

The above literature review shows that the Langmuir–Hinshelwood model has been frequently applied to characterize photocatalytic gas–solid surface processes using various substrate materials. On the other hand, to the authors' knowledge, the kinetics of photocatalytic acting concrete has not been analyzed so far.

Other relevant data on photocatalysis on concrete was found in [19]. Here, amongst other things, data is presented on the NO_x removal of a paving stone type (NOXER) which is exposed to varying NO concentrations. With the help of background information regarding the setup and conduction of measurement and analysis according to the Langmuir–Hinshelwood model, similar to the one above, was executed. The provided information about test setup and conditions were sufficient for adequate application of the model. In order to allow for a reproduction of the executed computations the boundary conditions are briefly given in the following as being extracted from [19]. The volumetric pollutant flow Q and the length of the sample (reactor) L amount to 3 l/min and 200 mm, respectively. The slit height h of the reactor was assumed to be 3 mm. As shown before, the analysis is not sensitive to this measure anyway. The relative humidity is given with 50% and the irradiance amounts to 6 W/m^2.

Using the data on the NO_x removal rate given in Table 4, a linear fit is derived as given in Fig. 3. It can be seen that the resulting data points fit well into the proposed model. Note that here, in difference to Fig. 2, only the NO concentration is varying but volumetric flow and slit height are maintained the same.

Based on these values, again conversion rate and adsorption equilibrium constant can be derived. For the given data, k amounts to 3.54 mg/m^{3}s and K_d to 0.538 m^3/mg, respectively. Compared to the previously discussed own experiments, the conversion rate constant is notably higher and vice versa the adsorption equilibrium rate constant smaller. On the conversion side this can be explained with different amounts and types of catalyst (anatase type) whereas the diffusion could be influenced by different surface morphology of the paving stones. The ratio of conversion/diffusion rates therefore amounts to 0.457 for the NOXER case, though the conversion rate is still more than twice the diffusion rate, it is less dominant now.

4. Extension of the model

In the former paragraph a general model for the reaction kinetics of heterogeneous photocatalytic oxidation on concrete substrates has been derived. This model contains the reaction kinetics and flow related parameters such as reactor dimension, volumetric flows and pollutant concentration. The difficulty of predicting the performance of a photocatalytic cementitious system including all pertinent factors lies in the large number of variables involved. However, for a comprehensive modeling at least two more external influences on the degradation efficiency have to be included into the model. These are the irradiance and the water vapor concentration, expressed by the relative humidity. Using these two influencing factors, the impact of changing weather conditions can be accounted for by the model.

4.1. Irradiance

The degradation process of NO molecules is caused by the photocatalytic activity of the catalyst surface. This photocatalytic behavior results from the optoelectronic properties of the used semiconductor. For the deployed catalyst (titanium dioxide in the anatase modification), the UV-A light ($\lambda<380$ nm) shows the most suitable range regarding the wavelength λ to start the photocatalytic oxidization. However, not only the wavelength is influencing the efficiency of the system, but also the light intensity or irradiance E has an effect on the degradation rate.

According to [20], the increase in the photocatalytic activity caused by increased irradiance can be divided into two limiting cases: i) for $E\leq 250$ W/m² the degradation increases proportional to E (linear dependence) and ii) for $E>250$ W/m² the photocatalytic activity grows with the square root of E for high irradiance (square root dependence). At very low range of irradiance ($E<10$ W/m²), where the present study needs to be placed, the dependency, however, deviates from this linear relation.

Table 4
NO and NO_x removal rate for a concrete paving block.

NO concentration [ppm]	NO removal [mmol/m²12h]	NO_x removal rate [%]
0.05	0.2	89.6
0.1	0.4	88.9
0.2	0.8	90.6
0.5	2.0	88.4
1.0	3.7	82.3
2.0	6.1	68.0
5.0	10.0	44.3

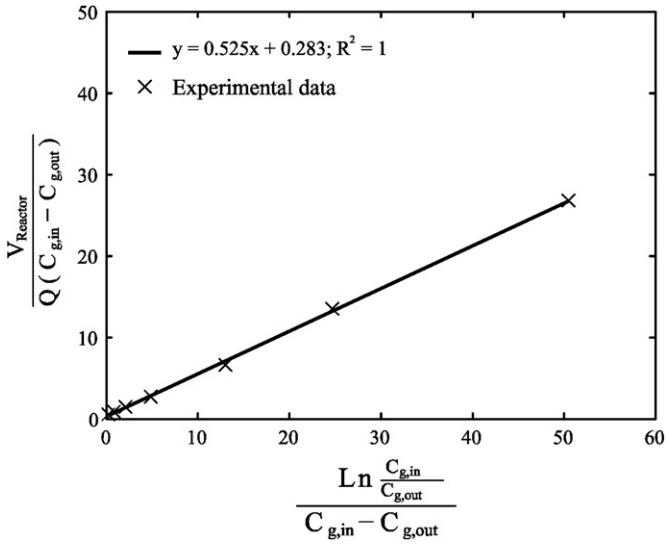

Fig. 3. Regression results of data presented in Table 4 for the photocatalysis of a NOXER paving block (data taken from [19]).

Now it is assumed that the irradiance only has an influence on the reaction rate constant k, while the adsorption equilibrium constant K_d remains unaffected. In order to validate this hypothesis an analysis similar to the one presented in Section 3.3 is carried out. Hereby for every state of irradiance, from 1 to 11 W/m^2 in steps of 1 W/m^2, a set of measurements varying the NO inlet concentration in steps of again 0.1, 0.3, 0.5, 0.7 and 1.0 ppmv is conducted (11×5 matrix). That means every value of K_d is represented by a linear fit similar to the one presented in Fig. 2, which again is based on 5 individual measurements (55 data points). A summary of all line fits ($y = mx + n$), used for the further analysis, is given in Table 5. From these line fits reaction rate constants and adsorption equilibrium rate constants can be determined in dependency of the respective irradiance level.

Fig. 4 shows the dependence of reaction rate constant k on the irradiance. The given function describes the relation between the irradiance and the achieved values of k for low values of irradiance (E<12 W/m²) adequately. The reaction rate constant k as a function of the irradiance E reads:

$$k = \alpha_1(-1 + \sqrt{1 + \alpha_2 E}), \tag{10}$$

with α_1 and α_2 being factors to be fitted from the experiment. This expression accounts for the linear and non-linear dependencies. When UV-radiation is absent, i.e. $E = 0$, the reaction rate becomes zero. For small E, Eq. (10) tends to become $\alpha_1\alpha_2 E/2$, and for large E it tends to $\alpha_1\sqrt{\alpha_2 E}$. As can be seen from Fig. 4, α_1 and α_2 have been

Table 5
Summary of all line fits for the derivation of k and K_d in dependency of varying irradiance.

Irrradiance level [W/m²]	Slope m	y-intercept n	k [mg/m^{3}s]	K_d [m^3/mg]	Coefficient of determination R²
1	2.2836	14.8450	0.07	6.50	0.6363
2	1.3924	9.9496	0.10	7.15	0.7524
3	1.4403	8.2467	0.12	5.73	0.8230
4	1.5596	6.3799	0.16	4.09	0.9185
5	1.3771	5.8175	0.17	4.22	0.9500
6	1.2885	5.1812	0.19	4.02	0.9567
7	1.2360	4.8082	0.21	3.89	0.9640
8	1.2035	4.3751	0.23	3.64	0.9663
9	1.1555	4.1155	0.24	3.56	0.9691
10	1.1074	3.9059	0.26	3.53	0.9694
11	1.0543	3.7483	0.27	3.56	0.9739

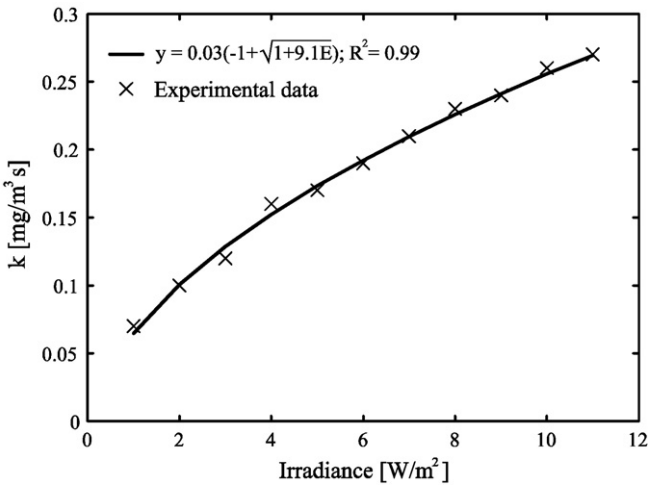

Fig. 4. Influence of UV-A irradiance on the reaction rate constant k, tested with constant $RH = 50\%$ and $C_{in} = 1.0$ ppmv NO.

fitted for the considered active paving stone and amount to 0.03 mg/m^{3}s and 9.1 m^2/W, respectively. Fig. 4 illustrates that Eq. (10) is in good agreement with the experimental results.

The influence of varying irradiance on the adsorption equilibrium constant K_d is demonstrated in Fig. 5. Not taking the first three measurements for very low values of irradiance into account, the initial hypothesis that the irradiance has no influence on the adsorption behavior is confirmed. Here a constant K_d of 3.81 m^3/mg can be derived for the respective paving stone sample. The first three outlying measurements represent very low irradiance levels where the light setup might not be stable enough. This concern is addressed in ongoing research. The disappearance rate of reactant from Eq. (7) hence is modified and now accounting for the influence of irradiance:

$$r_{NO} = \frac{K_{d,NO} C_{g,NO}}{1 + K_{d,NO} C_{g,NO}} \alpha_1(-1 + \sqrt{1 + \alpha_2 E}). \tag{11}$$

4.2. Relative humidity

The influence of the relative humidity depends to a large extent on the type of material used. According to [21], the hydrophilic effect at the surface is gaining over the oxidizing effect when high values of relative humidity are applied. The water molecules are adsorbed at

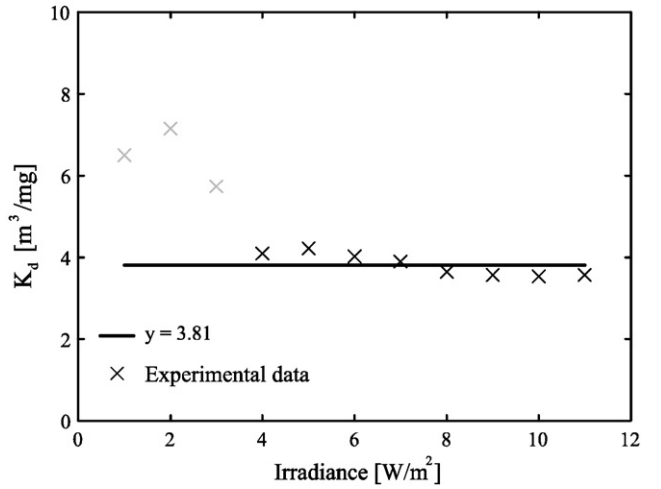

Fig. 5. Influence of UV-A irradiance on the adsorption equilibrium constant K_d, tested with constant $RH = 50\%$ and $C_{in} = 1.0$ ppmv NO.

the surface and prevent therefore the pollutants to adsorb on the reactive catalyst sites, which also is referred to in [17]. This could lead to the assumption that with increasing humidity the adsorption equilibrium constant K_d will be decreased. In other words, NO and water compete for free sites at the catalyst surface. Therefore, water vapor can be considered as an additional reactant. For reaction rates on mixtures of VOCs, [12] suggest an extended Langmuir–Hinshelwood model introducing additional reactants. For the present case this extended expression could consider the influence of humidity. Under consideration of the performed modifications from Eq. (11) the disappearance rate for the reactant NO, r_{NO}, would read:

$$r_{NO} = \frac{K_{d,NO}C_{g,NO}}{1 + K_{d,NO}C_{g,NO} + K_{d,H2O}C_{g,H2O}}\alpha_1(-1 + \sqrt{1 + \alpha_2 E}). \quad (12)$$

The water vapor concentration at 20 °C (experimental condition) and $RH = 100\%$ is 17.31 g/m^3, so that $K_{d,H2O}C_{g,H2O} = \alpha_3\ RH$ with $\alpha_3 = 17.31$ g/m^3 $K_{d,H2O}$. Furthermore, Eq. (12) can be rewritten as:

$$r_{NO} = \frac{K_d C_{g,NO}}{1 + K_d C_{g,NO}}\alpha_1(-1 + \sqrt{1 + \alpha_2 E}), \quad (13)$$

with K_d as effective adsorption equilibrium constant in the presence of water vapor:

$$K_d = \frac{K_{d,NO}}{1 + K_{d,H2O}C_{g,H2O}} = \frac{K_{d,NO}}{1 + \alpha_3 RH}, \quad (14)$$

Eq. (13) can be substituted into Eq. (8), which can be integrated, and with Eq. (5), again Eq. (9) is obtained, in which k is now a function of E and K_d of RH.

However, similar measurements as in the previous paragraph but now with varying the relative humidity (RH) in steps of 10% from 10% to 70% (7×5 measurement matrix), are not in line with the proposed model. The respective measurements are given in Fig. 6. These results learn that, against earlier expectations, there is no continuous decrease of NO adsorption with rising RH. It rather shows an optimum value of RH where the respective NO adsorption equilibrium achieves highest values. The dependence of K_d on the RH can be described with a polynomial equation of the second degree which reads as:

$$K_d = \alpha_4 RH^2 + \alpha_5 RH + \alpha_6, \quad (15)$$

The coefficients α_4, α_5 and α_6 have been fitted, and read for the present paving stone −0.001, 0.0802 and 1.63 m^3/mg, respectively.

Table 6
Summary of all line fits for the derivation of k and K_d in dependency of varying relative humidity.

Relative humidity [%]	Slope m	y-intercept n	k [mg/m^{3}s]	K_d [m^3/mg]	Coefficient of determination R^2
10	0.8936	2.0710	0.48	2.32	0.9917
20	0.9429	2.6468	0.38	2.81	0.9956
30	0.9974	3.1565	0.32	3.16	0.9967
40	1.1157	3.5380	0.28	3.17	0.9952
50	1.2941	3.9682	0.25	3.07	0.9910
60	1.6372	4.4894	0.22	2.74	0.9801
70	2.2471	5.0397	0.20	2.24	0.9775

The underlying line fits for all individual measurements are summarized in Table 6. Considering this specific sample, a level of RH at around 40% seems to be advantageous for a preferably high NO adsorption. The adsorption capacity of the pollutant onto the surface seems to be of major influence for the overall degradation performance of the NO. Therefore, a similar dependence of the NO degradation rate on the relative humidity is expected. However, measurements presented in Fig. 7 learn that this is not the case. Here, starting from 10% RH the degradation rate linearly decreases with increasing RH. This refers again the initial assumption of a sole influence of relative humidity on the adsorption equilibrium constant only. To obtain the linear behavior of NO degradation (cp. Fig. 7) while knowing the influence on the adsorption equilibrium constant (cp. Fig. 6) the reaction rate constant must have an influence, though. This is proven by the measurements given in Fig. 8. Considering the experimental data, the influence of the relative humidity on the reaction rate constant k can be explained by:

$$k = \alpha_7 RH^{\alpha_8}, \quad (16)$$

Again the coefficients α_7 and α_8 have been fitted and amount to 1.30 mg/m^{3}s and −0.42, respectively. The described behavior can be explained by the number of reaction sites which will be occupied by water molecules with increasing RH. Therefore, the more water vapor in the reactor the lower will be the degradation and the reaction rate constant, respectively, because of the lack of free reaction sites.

In conclusion it can be said that Eq. (9) cannot only be used to study the effects of C_{in} and Q, but also E and RH. From experimental data, α_1, α_2, α_7 and α_8 (all governing k), and α_4–α_6 (governing K_d) can be fitted. These fitting parameters finally allow the determination of k and K_d, which characterize each specific product. Using the

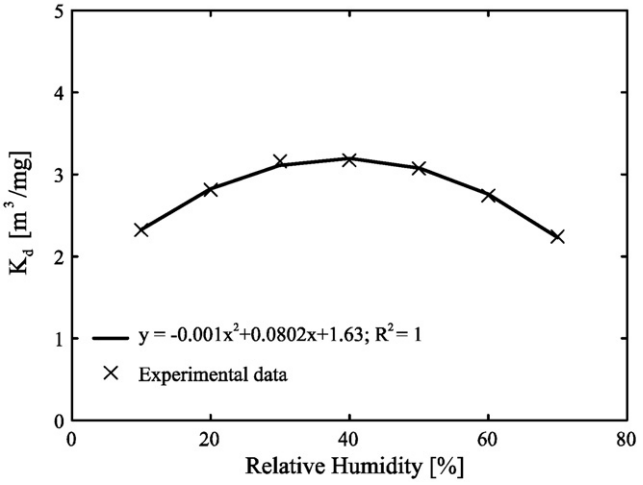

Fig. 6. Influence of relative humidity on the adsorption equilibrium constant K_d, tested with constant $E = 10$ W/m^2 and $C_{in} = 1.0$ ppmv NO.

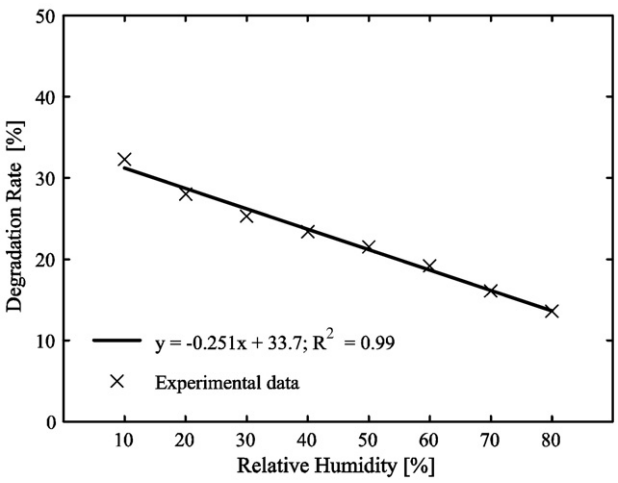

Fig. 7. Influence of relative humidity on the total NO degradation rate, tested with constant $E = 10$ W/m^2 and $C_{in} = 1.0$ ppmv NO.

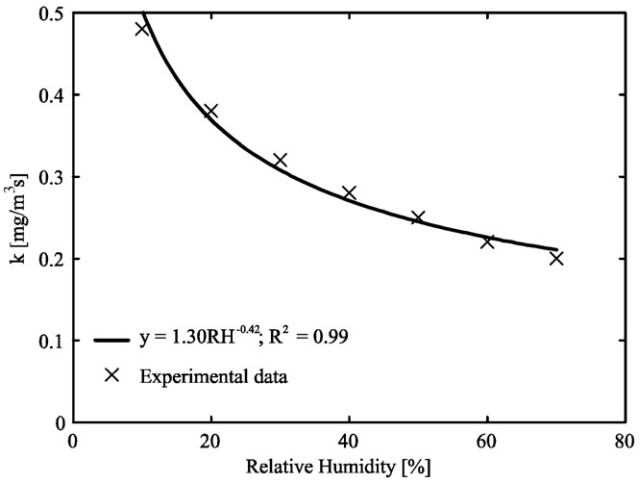

Fig. 8. Influence of humidity level on the reaction rate constant k, tested with constant $E = 10\ W/m^2$ and $C_{in} = 1.0$ ppmv NO.

disappearance rate of a reactant according to Eq. (7) the degradation rate can now be expressed in function of a varying irradiance at the relative humidity of 50% or, the other way around, in function of a varying relative humidity at an irradiance level of 10 W/m^2. A more complex derivation of the combined influences of irradiance and relative humidity on the disappearance rate is not possible with the present data. Such computations would require more measurement series with varying irradiance at relative humidity levels different from 50% and vice versa with irradiance levels different from 10 W/m^2.

5. Large-scale application

In general it can be concluded that PCO on concrete paving blocks is a proven reaction process which under controlled laboratory conditions can be highly effective. However, the demonstration of the same in real outside condition still seems to be a crucial point. Therefore, tests outside of the laboratory in a real street situation are necessary. If those tests can be concluded to be successful, their data can be used as input for real-scaled models in order to see whether the laboratory results can be translated to real site measurements.

In the recent past a few real site experiments have been conducted already. A central street for example was paved in Bergamo, Italy in 2006 [22]. Here a total area of 12,000 m^2 including road and sidewalk were paved with active paving blocks. This project was concluded to be successful. For the 10 h average of three consecutive days a decrease in NO_x-concentration of up to 30% was measured. Another, noteworthy project was the pavement of the sidewalks and parking lanes of road through the city center of Antwerp, Belgium [21]. Here a total area of 10,000 m^2 was paved. This project was successfully finished too, but specific data is not available which makes a further assessment difficult. Another major project is conducted now in Paris, France. In this case a heavily frequented road is paved with concrete containing TiO_2 as photocatalyst. Results are not published so far and a final report is expected later this year. There are some other case studies which are not specifically mentioned here. However, it can be concluded that so far no verifiable decrease of NO_x pollution can be specified, which originates solely on the action of the PCO provided by the photocatalytic characteristic of the pavement. This has a number of reasons which of the following are attached with greatest importance. In all cases there is no sufficient description of the initial pollutant situation given. This refers to the duration of measurements (possibly all seasons should be incorporated, annual mean) as well as to the positioning of the sample location. Here, especially the dilution of pollutant as a function of the distance to the source has to be accounted for. A representative measurement in the above sense of course also needs to be conducted after the respective surface is supplied with an active paving. Simultaneous comparative measurements need to be carried out in a similar but not treated environment (reference situation). Furthermore, should the location itself also show some aspects regarding the controllability of environmental influences. A “street-canyon” with close or even gap-free house construction in a straight and busy street seems to be favorable. But also the exposure to sunlight as well as the wind direction and velocity need to be considered for an analysis of the data.

Being aware of the insufficiencies of the above examples a new demonstration project was started in the second half of 2008. In the framework of this project a street ($170 \times 5.5\ m^2$) will be paved with active paving stones in the city of Hengelo, The Netherlands. In order to precisely describe the present situation comprehensive measurements are ongoing. Therefore, a protocol has been developed. The location is in accordance with the demands stated above. The measures which are monitored are the following: temperature, wind speed and wind direction, air pressure, relative humidity, NO concentration, NO_2 concentration, irradiance (visible and UV light), traffic volume, and ozone concentration. The direct measurements of the gaseous air pollutants are carried out at different locations (modified situation and parallel control-street with unchanged pavement) and in different heights above the ground (5 cm, 30 cm and 150 cm) in order to take account for the dilution effect. Furthermore, the measurements cover all seasons with each long lasting individual measurements. This way it is expected to gather valuable information on a large-scale change of the air quality. In addition, the results on the NO_x degradation in combination with the environmental parameters will be used as an input for computational fluid dynamics simulations (CFD) based on the reaction kinetics explained in the previous paragraph.

6. Conclusions

The heterogeneous photocatalytic oxidation is a promising technique for effectively reducing air pollution in inner city areas where high emissions of nitrogen oxides caused by increasing traffic loads are causing health problems. Besides this, the self-cleaning aspect coming along with PCO should not be ignored either. Concerning this matter, promising results have also been achieved, e.g. by [23,24].

Numerous measurements, also prior to this research project, carried out within the last two years showed that the concentration of nitrogen oxides in the ambient air can be notably reduced by the photocatalytic oxidation using TiO_2 under UV exposition. The experimental data obtained in a reactor provide a basis for the modeling of the degradation process using the Langmuir–Hinshelwood kinetics. The established model now allows for the prediction of the performance of certain air-purifying concrete products under various conditions. Due to the incorporation of the most important influencing boundary conditions namely pollutant concentration, volumetric flow, irradiance and relative humidity, a prediction of the degradation performance in a wide range is possible. Furthermore, now the unique characterization of photocatalytic concrete products is possible by the derivation of its conversion and adsorption rate constants. The derived model also confirms that in the considered reactor the conversion of NO_x is the rate-determining step in the photocatalytic oxidation of NO_x. The obtained modeling results are in a good agreement with the lab measurements.

Based on a thorough analysis of PCO on cementitious surfaces and the knowledge of its influencing parameters a reaction kinetics model was derived. With an ongoing on site experiment these models are now transferred to the real scale. Hereby representative measurements with sufficiently long measurement periods at modified as well as control locations are taken into account. For the associated computational fluid dynamics (CFD) calculations, the here derived kinetics will be used as it accounts for the effect of irradiance and relative humidity.

List of Symbols

Roman

B	breadth
C	concentration [mg/m^3, mole/mole, ppmv]
D	diffusion coefficient [m^2/s]
d_h	hydraulic diameter
E	irradiance [W/m^2]
h	height [m]
k	reaction rate constant [mg/m^{3}s]
K_d	adsorption equilibrium constant [m^3/mg]
L_d	critical length [m]
M	molecular mass [g/mole]
p	pressure [Pa]
Q	volumetric flow [l/min]
RH	relative humidity
r_x	disappearance rate of substance x
Sh	Sherwood number
T	temperature [K]
V	volume [m^3]
v	velocity [m/s]

Greek

ρ	density [g/cm^3]
λ	wavelength [nm]
υ	kinematic viscosity [m^2/s]

Subscript

con	converted
g	gas
h	hydraulic
NO	nitrogen monoxide
w	wall

Abbreviations

CFD	computational fluid dynamics
FEM	finite element analysis
NOM	natural organic matter
NIST	National Institute of Standards and Technology
PCE	perchloroethylene
PCO	photocatalytic oxidation
TCE	trichloroethylene
VOC	volatile organic compounds

Acknowledgements

This project was supported by the European Commission (6th FP Integrated Project "I-Stone", Proposal No. 515762-2). The authors furthermore wish to express their thanks to the following sponsors of their research group: Bouwdienst Rijkswaterstaat, Rokramix, Betoncentrale Twenthe, Graniet-Import Benelux, Kijlstra Beton, Struyk Verwo Groep, Hülskens, Insulinde, Dusseldorp Groep, Eerland Recycling, ENCI, Provincie Overijssel, Rijkswaterstaat Directie Zeeland, A&G maasvlakte, BTE, Alvon Bouwsystemen, and v. d. Bosch Beton (chronological order of joining).

References

[1] A. Fujishima, K. Honda, Electrochemical photolysis of water at a semiconductor electrode, Nature 238 (5358) (1972) 37.
[2] T.E. Doll, F.H. Frimmel, Photocatalytic degradation of carbamazepine, clofibric acid and iomeprol with P25 and Hombikat UV100 in the presence of natural organic matter (NOM) and other organic water constituents, Water Research 39 (2005) 403–411.
[3] C.C. Liu, Y.H. Hsieh, P.F. Lai, C.H. Li, C.L. Kao, Photodegradation treatment of azo dye wastewater by UV/TiO_2 process, Dyes and Pigments 68 (2–3) (2006) 191–195.
[4] G. Hüsken, M. Hunger, H.J.H. Brouwers, Comparative study on cementitious products containing titanium dioxide as photo-catalyst, in: P. Baglioni, L. Cassar (Eds.), Proceedings international RILEM symposium on photocatalysis, environment and construction materials-TDP 2007, RILEM Publications, Bagneux, 2007, pp. 147–154.
[5] L.P. Yang, Z.Y. Liu, H.W. Shi, H. Hu, W.F. Shangguan, Design consideration of photocatalytic oxidation reactors using TiO_2-coated foam nickels for degrading indoor gaseous formaldehyde, Catalysis Today 126 (3–4) (2007) 359–368.
[6] Y. Ku, C.M. Ma, Y.S. Shen, Decomposition of gaseous trichloroethylene in a photoreactor with TiO_2-coated nonwoven fiber textile, Applied Catalysis B-Environmental 34 (3) (2001) 181–190.
[7] H. Al-Ekabi, B. Butters, D. Delany, W. Holden, T. Powell, J. Story, The photocatalytic destruction of gaseous trichloroethylene and tetrachloroethylene over immobilized titanium dioxide, in: D.F. Ollis, H. Al-Ekabi (Eds.), Photocatalytic Purification and Treatment of Water and Air, Elsevier Science, Amsterdam, 1993, pp. 719–725.
[8] G. Imoberdorf, H.A. Irazoqui, A.E. Cassano, O.M. Alfano, Photocatalytic degradation of tetrachloroethylene in gas phase on TiO_2-Films: a kinetic study, Industrial and Engineering Chemistry Research 44 (16) (2005) 6075–6085.
[9] N. Fukami, M. Yosida, B.D. Lee, K. Taku, M. Hosomi, Photocatalytic degradation of gaseous perchloroethylene: products and pathway, Chemosphere 42 (4) (2001) 345–350.
[10] L.C. Burmeister, Convective heat transfer, John Wiley and Sons Inc, New York, 1993.
[11] M. Hunger, H.J.H. Brouwers, Self-cleaning surfaces as an innovative potential for sustainable concrete, in: M.C. Limbachiya, H.Y. Kew (Eds.), International conference excellence in concrete construction through innovation, 9–10 September 2008, London, United Kingdom, CRC Press, Balkema, Leiden, The Netherlands, 2009, pp. 545–552.
[12] J. Zhao, X.D. Yang, Photocatalytic oxidation for indoor air purification: a literature review, Building and Environment 38 (5) (2003) 645–654.
[13] Y. Dong, Z. Bai, R. Liu, T. Zhu, Decomposition of in-door ammonia with TiO_2-loaded cotton woven fabrics prepared by different textile finishing methods, Atmospheric Environment 41 (15) (2007) 3182–3192.
[14] R.K. Shah, A.L. London, Thermal boundary—conditions and some solutions for laminar duct flow forced convection, Journal of Heat Transfer 96 (2) (1974) 159–165.
[15] D.F. Ollis, Photoreactors for purification and decontamination of air, in: D.F. Ollis, H. Al-Ekabi (Eds.), Photocatalytic purification and treatment of water and air, Elsevier Science, Amsterdam, 1993, pp. 481–494.
[16] H.Q. Wang, Z.B. Wu, W.R. Zhao, B.H. Guan, Photocatalytic oxidation of nitrogen oxides using TiO_2 loading on woven glass fabric, Chemosphere 66 (1) (2007) 185–190.
[17] S. Devahasdin, C. Fan Jr., K. Li, D. Chen, TiO_2 photocatalytic oxidation of nitric oxide: transient behavior and reaction kinetics, Journal of Photochemistry and Photobiology A: Chemistry 156 (2003) 161–170.
[18] S. Matsuda, H. Hatano, A. Tsutsumi, Ultrafine particle fluidization and its application to photocatalytic NO_x treatment, Chem. Eng. Jour. 82 (1–3) (2001) 183–188.
[19] Mitsubishi Materials Corporation, NOx removing paving block utilizing photocatalytic reaction, in brochure: Noxer – NOx removing paving block, 2005.
[20] J.M. Herrmann, L. Péruchon, E. Puzenat, C. Guillard, Photocatalysis: from fundamentals to self-cleaning glass application, in: P. Baglioni, L. Cassar (Eds.), Proceedings international RILEM symposium on photocatalysis, environment and construction materials-TDP 2007, RILEM Publications, Bagneux, 2007, pp. 41–48.
[21] A. Beeldens, Air purification by road materials: results of the test project in Antwerp, in: P. Baglioni, L. Cassar (Eds.), Proceedings international RILEM symposium on photocatalysis, environment and construction materials-TDP 2007, RILEM Publications, Bagneux, 2007, pp. 187–194.
[22] G.L. Guerrini, E. Peccati, Photocatalytic cementitious roads for depollution, in: P. Baglioni, L. Cassar (Eds.), Proceedings international RILEM symposium on photocatalysis, environment and construction materials-TDP 2007, RILEM Publications, Bagneux, 2007, pp. 187–194.
[23] L. Cassar, A. Beeldens, N. Pimpinelli, G.L. Guerrini, E. Peccati, Photocatalysis of cementitious materials, in: P. Baglioni, L. Cassar (Eds.), Proceedings international RILEM symposium on photocatalysis, environment and construction materials-TDP 2007, RILEM Publications, Bagneux, 2007, pp. 131–145.
[24] G.L. Guerrini, A. Plassais, C. Pepe, L. Cassar, Use of photocatalytic cementitious materials for self-cleaning applications, in: P. Baglioni, L. Cassar (Eds.), Proceedings international RILEM symposium on photocatalysis, environment and construction materials-TDP 2007, RILEM Publications, Bagneux, 2007, pp. 219–226.